Design considerations for patient-specific bone fixation plates
a literature review

Brouwer de Koning, S. G.; de Winter, N.; Moosabeiki, V.; Mirzaali, M. J.; Berenschot, A.; Witbreuk, M. M.E.H.; Lagerburg, V.

DOI
10.1007/s11517-023-02900-4

Publication date
2023

Document Version
Final published version

Published in
Medical and Biological Engineering and Computing

Medical & Biological Engineering & Computing
https://doi.org/10.1007/s11517-023-02900-4

REVIEW ARTICLE

Design considerations for patient-specific bone fixation plates: a literature review

S. G. Brouwer de Koning[1] · N. de Winter[1] · V. Moosabeiki[2] · M. J. Mirzaali[2] · A. Berenschot[3] · M. M. E. H. Witbreuk[4] · V. Lagerburg[1]

Received: 22 April 2023 / Accepted: 29 July 2023

Abstract

In orthopedic surgery, patient-specific bone plates are used for fixation when conventional bone plates do not fit the specific anatomy of a patient. However, plate failure can occur due to a lack of properly established design parameters that support optimal biomechanical properties of the plate.

This review provides an overview of design parameters and biomechanical properties of patient-specific bone plates, which can assist in the design of the optimal plate.

A literature search was conducted through PubMed and Embase, resulting in the inclusion of 78 studies, comprising clinical studies using patient-specific bone plates for fracture fixation or experimental studies that evaluated biomechanical properties or design parameters of bone plates. Biomechanical properties of the plates, including elastic stiffness, yield strength, tensile strength, and Poisson's ratio are influenced by various factors, such as material properties, geometry, interface distance, fixation mechanism, screw pattern, working length and manufacturing techniques.

Although variations within studies challenge direct translation of experimental results into clinical practice, this review serves as a useful reference guide to determine which parameters must be carefully considered during the design and manufacturing process to achieve the desired biomechanical properties of a plate for fixation of a specific type of fracture.

Keywords Bone plate · Fracture fixation · Patient-specific · Biomechanical properties · Orthopedics

1 Introduction

In the field of orthopedic surgery, plates play a vital role in fixating bones following traumatic injuries or osteotomies. These plates not only provide rigid fixation and accurate repositioning of the fractured parts, but also apply compressive stress and strain at the fracture site to stimulate bone healing [1–3]. During load bearing, plates need to maintain the fractured ends in position while appropriately distributing the load exposed to the fracture. The plate should also allow for more accurate distribution of mechanical signals (*i.e.,* compressive stress and strain) to promote bone healing and bone density adaptation. The plate should prevent stress shielding, that may occur when the plate handles most of the load, and the density of the bone declines [4, 5]. Furthermore, tight fixation of the plate to the bone may affect blood supply, leading to necrosis [6, 7]. To achieve stable bone fixation with satisfactory bone union and complete functional outcome, it is essential to consider the biomechanical requirements during plate design and manufacturing.

Currently, orthopedic surgeons rely primarily on conventional bone plates, which are manufactured using computer numerical control (CNC) techniques in standard shapes and sizes, allowing for immediate use in emergency surgeries and cost-effective production [8, 9]. These plates are

S. G. Brouwer de Koning and N. de Winter contributed equally to this work.

✉ V. Lagerburg
v.lagerburg@antoniusziekenhuis.nl

1 Medical Physics, OLVG Hospital, Oosterpark 9, 1091 AC Amsterdam, The Netherlands

2 Department of Biomechanical Engineering, Faculty of Mechanical, Maritime, and Materials Engineering, Delft University of Technology, Delft, The Netherlands

3 Medical Library, Department of Research and Epidemiology, OLVG Hospital, Amsterdam, The Netherlands

4 Orthopedic Surgery, OLVG Hospital, Amsterdam, The Netherlands

typically made of biocompatible metals, such as titanium alloys or stainless steel, which can be sterilized and can withstand high loads [10, 11]. The conventional bone plates are an accepted solution with mostly satisfactory outcomes [10]. Despite this, they are not patient-specific and therefore do not precisely match individual anatomy. In some cases, they can be bent during surgery to improve the fit, but biomechanical or anatomical mismatch can still occur, leading to stress concentration and increasing the risk of plate or screw failure, or bone malunions [2]. In such instances, revision surgery may be required [12–15].

Computer-aided-design/computer-aided-manufacturing (CAD/CAM) techniques offer a solution to the mismatch between conventional bone plates and the patient's specific anatomy associated with complex fractures or osteotomies [12, 16]. Using computed tomography, digital three-dimensional (3D) models of the patient's anatomy can be developed to virtually plan the surgery and design bone plates that fit the patient's anatomy precisely. These patient-specific bone plates can be manufactured, for example by 3D-printing, and can be used during surgery [16–19].

In order to achieve optimal bone-plate fixation, it is crucial to optimize the biomechanical properties of the patient-specific bone plate. Such properties include load distribution, elastic stiffness, Poisson's ratio, yield strength and tensile strength [5, 20]. The consideration of these properties is imperative for ensuring the mechanical stability and durability of bone-plate fixation. The modification of these biomechanical properties can be achieved by tuning several parameters, including the type of material, screw type, number of screws, position of screws, plate geometry, working length, and gap between the bone and the plate. This literature review provides an overview of design parameters and their impact on biomechanical properties of patient-specific bone plates, to support designers to achieve the desired biomechanical properties for successful bone fixation.

2 Methods

A literature search was conducted in the PubMed and Embase databases on September 16th, 2020, and subsequently updated on July 6th, 2023 (PubMed) and July 14th, 2023 (Embase). The search strategy included both indexed and free terms related to computer-aided design, 3D-printing, and patient-specific bone plates, which were used to construct search queries. The resulting database was then deduplicated. Figure 1 shows the process for study selection.

Studies that investigated the use of patient-specific bone plates for fracture fixation or evaluated design parameters through biomechanical testing or finite element analysis (FEA) were included. References of included articles were screened on eligibility for inclusion. Studies that were not medical or studies in which plates were not used for fixation, were excluded. In addition, studies that did not assess plate design or did not provide information on the design of the plate, were excluded. In addition, studies that focused on surgical guides, implants, screws, or total replacements were excluded. Clinical studies that utilized conventional, rather than patient-specific bone plates, were ineligible. Also, studies that evaluated conventional bone plates that were pre-bent during surgery, or that presented operative techniques were excluded. Furthermore, studies related to maxillofacial, cranial, and animal studies were excluded. Finally, letters to the editor, review articles, conference abstracts, and studies not available in English were also excluded.

The included studies were systematically categorized according to various parameters that impact the biomechanical properties of the patient-specific bone plates, including material type, geometry, fixation mechanism and manufacturing techniques. Also, reported complications from relevant clinical studies were collected and analyzed.

3 Results

The initial search yielded a total of 1,428 articles. Through screening of article titles and abstracts, 1,098 articles were excluded. Full texts were not available of 28 records. Subsequently, the full texts of 302 studies were assessed, resulting in the inclusion of 74 articles, with an additional four identified through reference screening. Of these, 19 articles were clinical studies, while 59 described experimental studies focusing on biomechanical testing or FEA.

Experimental and FEA studies were conducted to analyze the relationship between design parameters and mechanical properties. The experimental studies included quasi static and dynamic biomechanical load tests on patient-specific bone plates, using techniques such as axial compression, three-point bending, four-point bending, torsion, tensile testing, and simulations of muscle forces. Literature on patient-specific bone plates described a range of biomechanical properties, including load distribution, Young's modulus, Poisson's ratio, yield strength and tensile strength. Design parameters related to the bone plate include material properties, geometry, fixation mechanism (with details such as working length, interface distance and screw pattern) and manufacturing technique.

3.1 Material

The plates were made of various biocompatible materials, including titanium, stainless steel, E-glass/epoxy composite, Carbon Fiber Reinforced PolyEtherEtherKetone (CFR-PEEK), glass fiber reinforced polypropylene, cobalt chromium (Co-Cr), cobalt chromium molybdenum (Co-Cr–Mo),

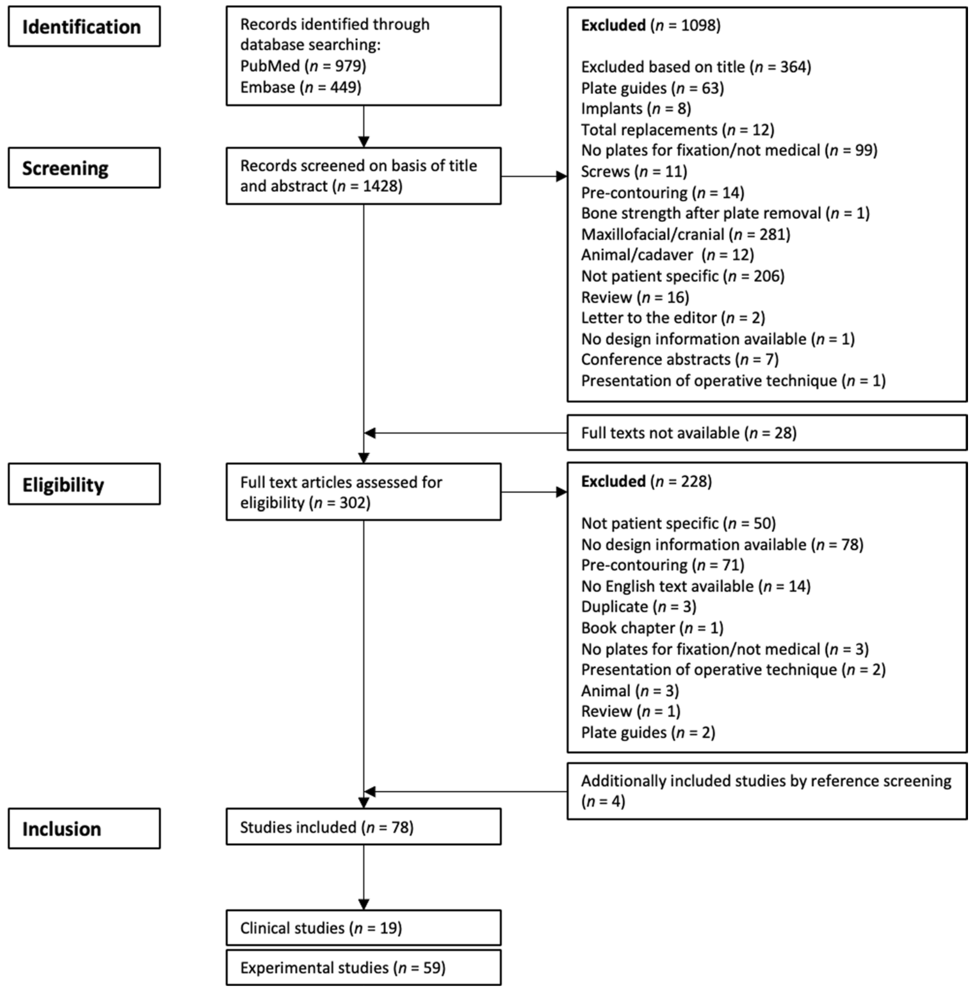

Fig. 1 Flow-chart of the literature search and study selection process

polylactic acid and nitinol (Table 1). Young's modulus, yield strength and ultimate tensile strength varied depending on the material, ranging from 1–280 GPa, 111–3,026 MPa, and 10–1,080 MPa, respectively. For example, titanium alloys had a Young's modulus of 105–193 GPa, a yield strength of 140–3,026 MPa and an ultimate tensile strength of 964–1080 MPa. The literature included patient-specific bone plate fixation in various parts of the body, including the femur, tibia, radius, ulna, humerus, spine, pelvis, clavicle and foot. Poisson's ratio, reported by 43 studies, ranged from 0.3 to 0.35 with a median 0.3.

3.2 Geometry

Literature on patient-specific bone plates provided information on the geometry of the plates, including shape, length, width, and thickness (Table 2). The shape of the plates varied based on the type of bone. For femur fixation, plate length ranged from 65- to 250-mm, whereas the width ranged from 8- to 35-mm and thickness ranged from 2- to 8-mm. For tibia fixation, plate length, width, and thickness ranged from 110- to 180-mm, 4.5- to 25-mm, and 2.5- to 6-mm, respectively. Pelvis plates had a thickness ranging from 3- to 3.5-mm, whereas plates for humerus fixation ranged in thickness from 2- to 4.5-mm. Radius plates were designed with a thickness ranging from 1.9- to 2.5-mm. For the rest of the bone types, only a few studies reported on geometry of the plates (Table 2).

3.3 Fixation

Studies investigating the biomechanical properties of patient-specific bone plates focused on fixation mechanisms for various bones (*e.g.,* femur, tibia, pelvis, humerus, radius, wrist, clavicle, spine and ulna) as documented in Table 3.

The plates were categorized into three main types based on their fixation mechanism: locking plates (LP), dynamic compression plates (DCP) and locking compression plates (LCP). LPs use threaded screw holes to lock the plate to the bone, while DCPs use non-threaded screw holes to allow for compressive loads [49]. LCPs feature both locking and compression screw holes, giving the surgeon

Table 1 Biomechanical properties of bone plate materials reported in the literature based on experimental testing or finite element analysis (FEA)

Author, year	*Type*	*Bone type*	*Young's modulus (Gpa)*	*Poisson's ratio*	*Yield strength (MPa)*	*Tensile strength (MPa)*	*Experimental biomechanical testing*	*FEA*
Titanium								
Caiti et al., 2019 [1]	Ti6A14V	Radius	110	0.35	1060			Axial compression; Bending moments; Torsion
Chen et al., 2018 [2]	Ti6A17Nb	Femur	123	0.3				Axial compression
Chen et al., 2023 [21]		Spine			919		Static compression test	
Chung et al., 2018 [22]		Femur	110	0.3				Axial compression; Torsion
Fan et al., 2017 [12]	Ti6A14V	Femur	115	0.3	800			Muscle forces
Freitas et al., 2021 [23]		Femur	193	0.33				Axial compression
Gupta et al., 2021 [24]	Ti6A14V	not specified			743	964	Tensile and 3 point bend tests	
Kaymaz et al., 2022 [25]	Ti6A14V	Humerus	110	0.31			Compression testing	Compression in x-, y- and z-direction
Kim et al., 2017 [26]	Ti6A14V	Radius			783–1114		Axial compression	
Kimshal et al., 2015 [27]		Tibia	110	0.34	207			Axial compression
Lin et al., 2018 [28]	Ti6A14V				862	910	4 point bending test	
Liu et al., 2014 [10]	Ti6A14V	Clavicle			1347–3026		4 point bending test	
Macleod et al., 2018 [29]	Ti6A14V	Tibia			789–1013		Axial compression	Muscle forces
Munch et al., 2022 [30]		Tibia	110	0.3			Compression testing	Medial–lateral compression
Samsami et al., 2022 [31]		Tibia					Quasistatic and cyclic loading	
Schader et al., 2022 [32]		Humerus	105	0.3				Shoulder abduction and flexion in several degrees
Shams et al., 2022 [33]	Ti6A14V	Femur	113,8	0.33	839.9			Axial compression
Smith et al., 2016 [8]	Ti6A14V ELI	Foot			877–897	916–937	3 point bending test	
Sokol et al., 2011 [34]		Radius				472–826	Axial compression	
Soni et al., 2020 [35]	Ti6A14V	Femur	110	0.33	825	1080		Axial compression
Subasi et al., 2023 [36]	Ti6A14V		105	0.33	1137			Axial compression
Stoffel et al., 2003 [37]			115	0.34			Axial compression; Torsion	Axial compression; Torsion

Table 1 (continued)

Author, year	*Type*	*Bone type*	*Young's modulus (Gpa)*	*Poisson's ratio*	*Yield strength (MPa)*	*Tensile strength (MPa)*	*Experimental biomechanical testing*	*FEA*
Synek et al., 2021 [38]		Radius	105	0.34				Axial compression
Reina-Romo et al., 2014 [39]	Ti6A17Nb	Femur	123	0.31				Muscle forces
Thomrungpiyathan et al., 2021 [40]	Ti6A14V	Humerus	110	0.34	1025			Axial compression
Tseng et al., 2016 [11]	Ti6A14V	Femur	110	0.3			4 point bending test	4 point bending test
Vancleef et al., 2022 [41]	Ti6A14V	Clavicle	115	0.3				Unloaded and loaded anteflexion and abduction
Wang et al., 2017 [42]	Ti6A14V	Pelvis			900	1000	Hardness	
Wang et al., 2020 [43]	Ti6A14V	Tibia	110	0.3				700 N for fulll weight bearing
Wang et al., 2022 [44]	Ti6A14V	Spine	110	0.3				Axial compression
Wee et al., 2017 [45]		Femur	110	0.3			Axial compression; Torsion	Axial compression; Torsion
Yao et al., 2021 [46]		Foot	110	0.3				Axial compression
Zhang et al., 2019 [47]		Clavicle	186,4	0.3	140			Axial compression
Stainless steel								
Chakladar et al., 2016 [48]		Ulna	280	0.33			3 point bending test	3 point bending test
Chung et al., 2018 [22]		Femur	210	0.3				Axial compression; Torsion
Fan et al., 2018 [12]		Femur	196	0.33	310			Muscle forces
Kanchanomai et al., 2010 [49]	316L	Femur	193			595	Axial compression; 4 point bending test	
Kimshal et al., 2015 [27]	316L	Tibia	205	0.3	207			Axial compression
Murat et al., 2021 [50]		Humerus	193	0.3			Axial compression	Axial compression
Olender et al., 2011 [51]	AISI 304		193	0.3			4 point bending test	4 point bending test
Peleg et al., (2006) [52]		Femur			111		Axial compression	Axial compression
Reina-Romo et al., 2014 [39]	316L	Femur	193	0.3				Muscle forces
Soni et al., 2020 [35]	316L	Femur	200	0.3	290	580		Axial compression
Stoffel et al., 2003 [37]			220	0.34			Axial compression; Torsion	Axial compression; Torsion

Table 1 (continued)

Author, year	*Type*	*Bone type*	*Young's modulus (Gpa)*	*Poisson's ratio*	*Yield strength (MPa)*	*Tensile strength (MPa)*	*Experimental biomechanical testing*	*FEA*
Teo et al., 2022 [53]	316L	Tibia					Loaded cyclically from 100 N to 3 times body weight	
Tilton et al., 2020 [9]	316L	Humerus	193	0.3			Axial compression; Torsion	Axial compression; Torsion
Tseng et al., 2016 [11]	F138, F1314	Femur	200	0.3			4 point bending test	4 point bending test
Wee et al., 2017 [45]		Femur	200	0.3			Axial compression; Torsion	Axial compression; Torsion
Yan et al., 2020 [54]	316L	Tibia	193	0.3	690	860		Axial compression
Other								
Chakladar et al., 2016 [48]	E-glass/epoxy composite	Ulna	15	0.3			3 point bending test	3 point bending test
Chung et al., 2018 [22]	CFR-PEEK	Femur	50	0.3				Axial compression; Torsion
Kabiri et al., 2021 [55]	Glass fiber reinforced polypropylene	Tibia	1–20,1	0.1–0.35		10–400	Density, tensile, compression, four-point bending, shear and Charpy impact resistance tests	
Le et al., 2023 [56]	Polylactic acid					72	Tensile and 4 point bending	
Nobari et al., 2010 [57]	Cobalt-chromium	Femur	200	0.3				Mediolateral and anteropostero force; Axial compression
Ren et al., 2022 [58]	not specified	Tibia	110	0.3				Axial compression
Soni et al., 2020 [35]	Co-Cr-Molybdenum	Femur	100	0.3	450	720		Axial compression
Olender et al., 2011 [51]	Nitinol		23	0.33			4 point bending test	4 point bending test
Wang et al., 2020 [59]	not specified	Femur	200	0.3				Axial compression

greater flexibility to determine the optimal approach for each case [49]. All three types of fixations were utilized for various types of bone (Table 3). Pelvic fixation primarily used dynamic compression, while locking fixation was dominant in radius fixation. Clinical studies also evaluated all three types of plates across different types of bone.

The interface distance, *i.e.*, the distance between bone and plate after fixation, reported in literature ranged from 0.0 to 6.0 mm (Table 3).

Studies investigated surgical outcomes using different screw patterns (*e.g.*, straight in line, triangular or alternating patterns). In particular, conventional bone plates with a standard arrangement of screw holes (Fig. 2a) were compared to plates with triangular patterns (Fig. 2b) or an alternating pattern of screws, in terms of yield strength and stress distribution [1, 54]. In addition, different screw configurations were tested using a conventional straight in-line arrangement of screw holes [39, 45, 48, 70]. The number

Table 2 Geometry of bone plates per bone type

Bone type	*Author, year*	*Shape*	*Recommended measures as a result of the research*		
			Length (mm)	*Width (mm)*	*Thickness (mm)*
Femur	Arnone et al., 2013 [60]				5.5
	Chen et al., 2018 [2]		126.6 ± 6.5		3
	Chen et al., 2017 [13]	Three different widths for proximal, middle and distal	132.1	17, 22.5, 34.5	2, 4, 5
	Chung et al., 2018 [22]		70	8	4
	Fan et al., 2017 [12]				4.75 (Titanium); 5.25 (Stainless steel)
	Kanchanomai et al., 2010 [49]		250		
	Nobari et al., 2010 [57]	Short, wide and thick	65	35	7–8
	Shams et al., 2022 [33]				5
	Tseng et al., 2016 [11]		130	18	5.05
	Wee et al., 2017 [45]			4.5	4
	CLINICAL: Ma et al., 2017 [61]				6
Tibia	Kabiri et al., 2021 [55]		110	25	5.5
	Kimshal et al., 2015 [27]	Short plates inferior to longer plates			3, 3.75
	Macleod et al., 2018 [29]	Thicker and wider around screw holes			
	Petersik et al., 2018 [20]				
	Ren et al., 2022 [58]	L-shaped			3.5
	Shin et al., 2022 [62]	Straight	149.5	12	2.5
	Wee et al., 2017 [45]			4.5	4
	Yan et al., 2020 [54]			5	
	Wang et al., 2020 [43]		180	14.4	4
	CLINICAL: Ma et al., 2017 [61]				6
No type specified	Ghimire et al., 2019 [63]		206	17.5	5.2
	Gupta et al., 2021 [24]	Straight	70	17.5	3
	Lin et al., 2018 [28]		140	18	5.05
	Olender et al., 2011 [51]	Dogbone: thin in middle of the plate	53	6	
	Stoffel et al., 2003 [37]				4.5
Pelvis	Wang et al., 2017 [42]			10	3–3.5
	Wen et al., 2020 [64]				3
	CLINICAL: Wang et al., 2020 [65]				3–3.5
Humerus	Ahmad et al., 2007 [66]				4.5
	Murat et al., 2021 [50]	Density variation in a porous plate			
	Thomrungpiyathan et al., 2021 [40]	Addition of a lateral brim with a lateral-medial linking screw	110	10	2
	Tilton et al., 2020 [9]				3.5
Radius	Caiti et al., 2019 [1]				1.9
	Kim et al., 2017 [26]				2.5
	Synek et al., 2021 [38]				2
Wrist	CLINICAL: Del Pino et al., 2014 [67]		94	6, 8.1	2.5
	CLINICAL: Sodl et al., 2002 [68]		104	6, 8	
Foot	Smith et al., 2016 [8]	Dogbone: thin in middle of the plate			
	CLINICAL: Yao et al., 2021 [46]	Increased bottom width			3.5

Table 2 (continued)

Bone type	*Author, year*	*Shape*	*Recommended measures as a result of the research*		
			Length (mm)	*Width (mm)*	*Thickness (mm)*
Clavicle	Liu et al., 2014 [10]				3.5
	Vancleef et al., 2022 [41]				1.5
Spine	Chen et al., 2023 [21]	H-shaped			0.6
	Peterson et al., 2018 [69]	Material removed from centre of the plate to lower stiffness			
	Wang et al., 2022 [44]	Palm-leaf fan-shaped	32	22	5
Ulna	Chakladar et al., 2016 [48]		78	9–12	4.25, 4.85

of screw holes used in patient-specific bone plates ranged from 3 to 16 (Table 3). For example in femur plates, it was recommended to use 2–5 screw holes on either side of the fracture. Of particular interest was the number of screws used on either side of the fracture, and the working length, which is defined as the length between the first screw at each side of the fracture. The latter ranged from 5 to 102 mm.

Some studies have made recommendations on optimal screw patterns and working length for specific bone types. For example, in femur fixation, several studies recommend a significant working length with limited use of screws close to the gap [22, 39, 49]. An optimal working length for tibia fixation ranged between 38.5- and 62.5-mm [30, 83]. Studies that did not specify the bone type recommend a significant working length and report on an increased flexibility in compression and torsion, with unused holes nearby the gap [37]. This can also reduce the number of screws used significantly [29]. For humerus fixation, at least three screws on each side of the fracture and an increased working length are recommended [9, 40]. In radius fixation, it was found that the number of screws can be reduced to three, with only minor reduction of stiffness and strain when choosing an optimized configuration [38] (Fig. 3).

3.4 Manufacturing techniques

Several studies have investigated manufacturing techniques for patient-specific bone plates, with five studies using conventional techniques in combination with milling ($n=4$) and one un-specified method (Table 4). Besides conventional manufacturing techniques, 3D printing techniques were evaluated in 17 studies for the manufacturing of plates with complex geometries, with various types of powder bed fusion techniques utilized, including selective laser sintering or melting ($n=11$), direct metal laser melting ($n=1$), electron beam melting ($n=2$), laser-based cutting and welding ($n=1$) and three un-specified methods. Post-processing steps were required for 3D printed plates to enhance fatigue strength and reduce surface roughness [8, 10, 63], with anodizing, polishing, heat treatment, roll casting, acid pickling, abrasive blasting and coating (Table 4). The manufacturing and post-processing time ranged from 24 h till 7 days.

3.5 Clinical complications

Clinical studies were conducted on various bone plate types, including the plates used for acetabulum/pelvis (104 patients), tibia (6 patients), wrist (30 patients), femur (8 patients), radius (24 patients) and humerus (19 patients). In these patients, patient-specific bone plates ($n=129$) and conventional bone plates ($n=65$) were used (Table 5). Mean age of the patients was reported to estimate the role of osteoporosis. Complications associated with patient-specific bone plates included pain of scar and surrounding tissue, infection, nerve injury, screw loosening, thromboembolism, heterotopic bone ossification, and reduced physical function. For conventional bone plates, complications included wound infection, deep vein thrombosis, traumatic arthritis, nerve injury, and decrease in physical function.

Two studies comparing patient-specific and conventional bone plates showed a decrease in mean surgery time when patient-specific bone plates were used [78, 91].

4 Discussion

In the field of orthopedic surgery, there is an increasing interest in the use of patient-specific bone plates to fixate bones, particularly when conventional plates do not precisely match individual anatomy. Although patient-specific plates are associated with safe outcomes, there is a risk of plate failure due to the lack of established design parameters that support optimal biomechanical properties of the plate. This literature review provides an overview of design parameters and discusses the impact of the design parameters on biomechanical properties of patient-specific bone plates, to assist designers in manufacturing optimal bone plates.

Table 3 Fixation mechanisms, interface distance, screw pattern, working length, and final optimized geometry categorized per bone type

Bone type	*Author, year*	*Fixation mechanism*	*Interface distance (mm)*	*Screw Pattern*	*Number of screw holes*	*Working length (mm)*	*Final optimization*
Femur	Arnone et al., 2013 [60]	Locking					
	Chung et al., 2018 [22]	Locking compression	0.0–2.0			5–40	Working length composite ≤ 20 mm vs titanium ≤ 15 mm vs steel ≤ 30 mm
	Fan et al., 2018 [12]	Locking	0.0; 1.0; 2.0				
	Freitas et al., 2021 [23]			Sliding hip screw, L-shaped and L-shaped with medial plate			Sliding hip screw and L-shaped with medial plate
	Kanchanomai et al., 2010 [49]	Locking compression			14	1) 2 holes closest to gap unused 2) 8 holes closest to gap unused	8 holes closest to gap unused
	Märdian et al., 2015 [70]	Locking		Different configurations of 4 proximal screws	13 proximal and 7 distal	42; 62; 82; 102	3 screws on either side
	Nobari et al., 2010 [57]				4–10		2–5 screw holes on either side
	Peleg et al., (2006) [52]	Dynamic compression		Distal	2; 4		Long plate; 4 distal screws
	Reina-Romo et al., 2014 [39]	Locking compression		Proximal: 3–6; Distal: 8	11–14	All holes used vs hole or 2 holes closest to gap unused	hole closest to gap unused with 4 proximal screws / 2 holes closest to gap unused with 3 alternating proximal screws
	Tseng et al., 2016 [11]	Locking			3		Non-threaded holes
	Wang et al., 2020 [71]	Dynamic compression		Straight	2-hole, 4-hole and 6-hole		4-hole or 6-hole
	Wang et al., 2021 [72]		0.16				
	Wee et al., 2017 [45]	Locking compression	1.0	various	8–16	various	
	CLINICAL: Ma et al., 2017 [61]	Locking					

Table 3 (continued)

Bone type	*Author, year*	*Fixation mechanism*	*Interface distance (mm)*	*Screw Pattern*	*Number of screw holes*	*Working length (mm)*	*Final optimization*
Tibia	Kabiri et al., 2021 [55]				6		
	Kimshal et al., 2015 [27]	Dynamic compression Locking					
	Macleod et al., 2018 [29]	Locking			7; 8	33; 50	7 screw holes; 50 mm working length
	Munch et al., 2022 [30]	Locking					
	Petersik et al., 2018 [20]	Locking compression	0.9–2.41		8; 9; 10; 12; 16		
	Samsami et al., 2022 [31]	Locking					
	Shin et al., 2022 [62]	non locking					
	Teo et al., 2021 [73]	Locking					
	Yan et al., 2020 [54]	Locking compression		Straight/alternating	6	2 holes closest to gap unused	Alternating pattern and 2 holes closest to gap unused
	Wang et al., 2020 [43]	Locking plate with locking and dynamic holes		Straight	8 or 10 holes	6.5 + 4 mm steps up to 62.5	Working length: > 38.5 mm and < 62.5 mm
	CLINICAL: Bastias et al., 2014 [74]	Dynamic compression Locking compression					
	CLINICAL: Ma et al., 2017 [61]	Locking					
	CLINICAL: Oraa et al., 2023 [75]			4 proximal and 5 distal			

Table 3 (continued)

Bone type	*Author, year*	*Fixation mechanism*	*Interface distance (mm)*	*Screw Pattern*	*Number of screw holes*	*Working length (mm)*	*Final optimization*
No type specified	Gardner et al., 2010 [76]	Locking compression Locking			10		Hole at gap unused and use of multi-holes
	Ghimire et al., 2019 [63]	Locking compression	0.0; 2.0; 4.0		11	30; 100	100 mm working length with interface distance ≤ 2 mm
	Lin et al., 2018 [28]	Locking			3		Half or 1/3 of screw threads removed
	Stoffel et al., 2003 [37]	Locking compression	2.0; 6.0	6; 8; 12 screws in various patterns	12	1) all holes used 2) 2 holes closest to gap unused 3) 4 holes closest to gap unused	3 screws on either side 2) twice as flexible compared to 1) in compression and torsion
Pelvis	Jo et al., 2023 [77]		0.407 +—0.342				
	Wang et al., 2017 [42]	Dynamic compression					
	Wen et al., 2020 [64]	Dynamic compression					
	CLINICAL: Wu et al., 2020 [78]	Dynamic compression					
	CLINICAL: Xu et al., 2014 [79]	Locking					
Humerus	Ahmad et al., 2007 [66]	Dynamic compression Locking compression	0.0; 2.0; 5.0		7		
	Murat et al., 2021 [50]			Straight	4		
	Schader et al., 2022 [32]	Locking		6 proximal screws with 3 shaft screws			Subject-specific optimization of screw orientation leads to lower cutout risk and improved fixation
	Thomrungpiyathan et al., 2021 [40]				5 plate screws with 2 medical-lateral screws		at least 3 screw fixations on each side of the fracture
	Tilton et al., 2020 [9]	Locking			12	2 holes closest to gap unused	2 holes closest to gap unused

Table 3 (continued)

Bone type	*Author, year*	*Fixation mechanism*	*Interface distance (mm)*	*Screw Pattern*	*Number of screw holes*	*Working length (mm)*	*Final optimization*
Radius	Caiti et al., 2019 [1]	Locking compression		Straight vs Triangular	9 vs 6		Triangular pattern, 6 screw holes
	Kim et al., 2017 [26]	Locking			11		Hole diameter of 2.5 mm
	Sokol et al., 2011 [34]	Locking			10		10 screw holes
	Synek et al., 2021 [38]	Locking		6, 5, 4, 3 distal screws			up to 3 screws could be removed with only minor reduction of stiffness and strain
	CLINICAL: Dobbe et al., 2014 [80]	Locking					
Wrist	CLINICAL: Del Pino et al., 2014 [67]	Locking compression					
	CLINICAL: Sodl et al., 2002 [68]	Dynamic compression					
Clavicle	Liu et al., 2014 [10]	Locking compression					
	Vancleef et al., 2022 [41]		0.47	screws were positioned equidistance from each other, maximally spread in each segment			
	Zhang et al., 2019 [47]	Locking		Straight	6		
Spine	Brodke et al., 2001 [81]	Dynamic compression Locking					
	Chen et al., 2023 [21]				4		
	Peterson et al., 2018 [69]	Dynamic compression			4		4 screw holes
	Wang et al., 2022 [44]	Locking			4		
Ulna	Chakladar et al., 2016 [48]	Locking compression	0.5	15 combinations of 6	8		Pattern I an IX (Fig. 15)
	Sharma et al., 2023 [82]	Locking					

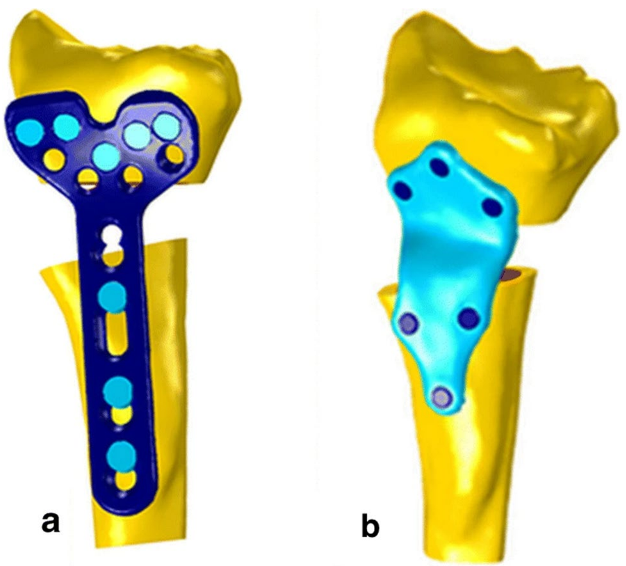

Fig. 2 **a** Conventional screw pattern **b** triangular screw pattern ((1), which is licensed under the Creative Commons Attribution 4.0 International License)

To ensure optimal biomechanical properties, the patient-specific bone plate should ideally resemble the properties of bone. The properties of a specific type of bone reflect its function in the skeleton, which is dependent on the loading conditions applied to that specific bone. Similarly, the design and properties of a bone plate must match the biomechanical requirements of the specific bone and loading conditions to achieve optimal fixation. In an ideal situation the bone plate is manufactured/3D-printed according to several parameters adjusted for the patient's specific situation: the expected load bearing, the type of bone that needs fixation, the health/age of the bone and the shape of the bone to provide a perfect fit. Physiological loading conditions on the plate vary per fixated bone, with higher loads to withstand for lower extremity plate fixation compared to upper extremity plate fixation. The daily life load ranges between 0.5 and 400% of the patient's bodyweight, for full weight bearing [22, 35, 66, 80]. It is essential to consider bone-specific Young's modulus when developing plates with biomechanical properties that match the type of bone for future purposes. Studies report a higher range of yield- and tensile strength for titanium alloys compared to stainless steel, indicating that titanium alloys can tolerate a higher maximum stress before undergoing plastic deformation and can withstand a higher stress before failing. Composite materials, in general, have a lower yield- and tensile strength, making them less suitable for fixating high load-bearing bones (*e.g.,* femur and tibia), and are therefore not used in clinical practice [48, 60]. Tantalum is a promising material which is studied mostly in experimental or animal studies so far. Liu et al. conducted an experimental study of a 3D-printed permanent implantable tantalum-coated Ti6A14V bone plate for fracture fixation [93]. The plate had an elastic modulus like cortical bone and no stress shielding occurred. The tantalum coating enhances the attachment and proliferation of cells on the surface. Fan et al. tested the biomechanical properties of 3D printed tantalum and titanium porous scaffolds. Under uniaxial-compression tests, equivalent stress of tantalum scaffold was significantly larger than the titanium scaffolds. With varying pore diameters, they succeeded to produce stress–strain curves of tantalum scaffolds more like pig bone scaffolds than titanium scaffolds [94].

Stress shielding occurs when the applied load is passed on via the bone plate instead of the bone itself. This hampers bone remodeling and the healing process via callus formation and leads to loosening of the plate and union deformities. Stress shielding is caused by the mismatch in stiffness between the bone plate and the bone itself. To prevent this,

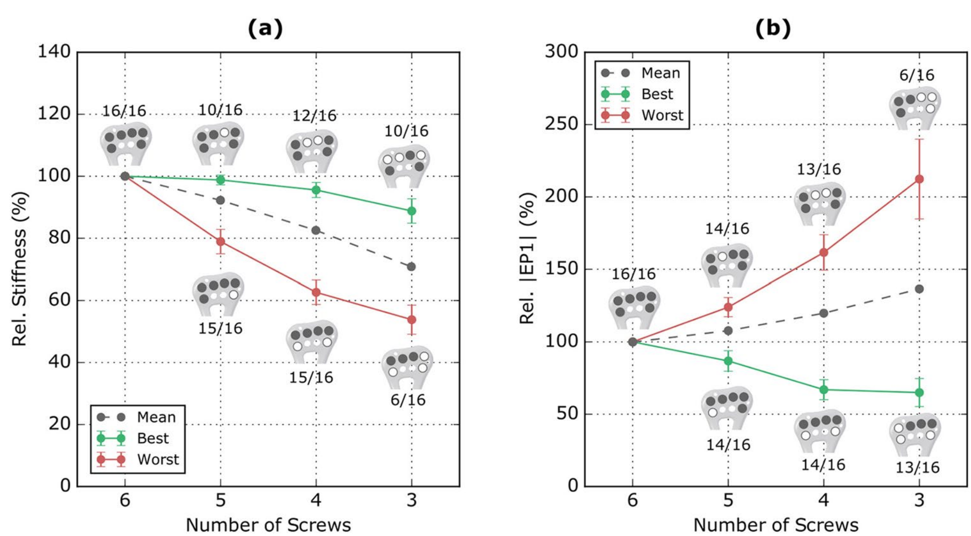

Fig. 3 Best and worst configurations for each number of screws with respect to axial stiffness **a** and peri-implant strains **b** related to the number of subjects (10/16 means in 10 out of 16 subjects) ((33), which is licensed under the Creative Commons Attribution 4.0 International License)

Table 4 Manufacturing- and post-processing methods per bone type

Bone type	*Author, year*	*Manufacturing method*	*Post-processing*	*Time to develop*
Femur	CLINICAL: Ma et al., 2017 [61]	CNC with milling	Polishing; Anodizing	
Tibia	Kabiri et al., 2021 [55]	Hot press or 3D print		
	Macleod et al., 2018 [29]	Selective laser sintering		
	Shin et al., 2022 [62]	Powder bed fusion	removal of supporter, surface finishing using hand piece and blasting with ceramic microbeat	
	Teo et al., 2021 [73]	Selective laser melting		24 h and 7 min
	Teo et al., 2022 [53]		Support removal and beat blasting	24 h
	CLINICAL: Jeong et al., 2022 [84]	3D print		
	CLINICAL: Ma et al., 2017 [61]	CNC with milling	Polishing; Anodizing	
	CLINICAL: Oraa et al., 2023 [75]	Selective laser melting		
No type specified	Gupta et al., 2021 [24]	Selective laser melting	repeated cyclic heating and cooling below the ß-transus temperature, and milling	
	Le et al., 2023 [56]	Fused deposion modelling, 0.1 mm layer height		
	Olender et al., 2011 [51]	Laser cutting and welding		
Pelvis	Jo et al., 2023 [77]	Powder bed fusion	Blasting with ceramic microbeads	Approx. 5 h
	Wang et al., 2017 [42]	Selective laser melting	Vacuum heat treatment; Anodizing	24 h
	Wen et al., 2020 [64]	Selective laser melting		
	CLINICAL: Ijpma et al., 2021 [85]	5-axes milling		<4 days
	CLINICAL: Merema et al., 2017 [86]	CNC with milling		3 days
	CLINICAL: Wang et al., 2020 [65]	Selective laser melting; CNC	Heat treatment; Roll casting; Acid pickling; Polishing; Anodizing	3.5 days
	CLINICAL: Xu et al., 2014 [79]	CNC with milling	Polishing; Anodizing	
Humerus	Kaymaz et al., 2022 [25]	Selective laser melting		
	Murat et al., 2021 [50]	Selective laser melting		
	Thomrungpiyathan et al., 2021 [40]	Selective laser melting	Heat treatment	3–5 days
	Tilton et al., 2020 [9]	Laser powder bed fusion with forging	Heat treatment	13 h
Radius	Kim et al., 2017 [26]	Direct metal laser melting	Abrasive blasting with zirconia	13 h
Ulna	Sharma et al., 2023 [82]	Fused filament fabrication	Coated with polydopamine	
Clavicle	Liu et al., 2014 [10]	Electron beam melting		
Foot	Edelmann et al., 2020 [87]	Selective laser melting	Stress relief annealing	
	Smith et al., 2016 [8]	Selective laser melting	Polishing; Anodizing	
	CLINICAL: Yao et al., 2021 [46]	Electron beam melting	Trimmed, polished and anodized	3–7 days

some studies have attempted to reduce the materials' stiffness to approximate that of bone. For example, Yan et al. performed a material sweep in FEA to reduce the elastic stiffness of a stainless-steel plate (with an original elastic stiffness of 193 GPa) to an elastic stiffness more closely resembling bone. When subjected to 100% body weight, a plate with an elastic stiffness of 20 GPa failed, while a 50 GPa plate was the limit of failure [54]. Composite materials have also been investigated to reduce plate (elastic) stiffness. Chakladar et al. reported a composite (E-glass/epoxy composite) with an elastic stiffness within 8% of bone (elastic) stiffness, in theory strong enough to allow for ulnar fixation but not for high weight-bearing bone types [48].

Poisson's ratio characterizes the deformation of a plate in response to strain and has an average value of 0.3 for both cortical and cancellous bone [1, 2, 9, 22, 27, 29, 37, 39].

Table 5 Clinical studies reporting on patient-specific bone plates used in patients with reported number of patients, mean follow-up, postoperative complications and mean surgery time

Bone type	*Author, year*	*Patient-specific/ conventional*	*Number of patients*	*Mean age (years)*	*Mean follow-up (months)*	*Postoperative complications*	*Mean surgery time (min)*
Femur	Ma et al., 2017 [61]	Patient-specific	8	22.8	29.3	1 infection and 1 nerve injury	272
Tibia	Jeong et al., 2022 [84]	Patient-specific	1	38	1.5	None	65
	Ma et al., 2017 [61]	Patient-specific	4	22.8	29.3	1 infection and 1 nerve injury	272
	Oraa et al., 2023 [75]	Patient-specific	1	43	5	None	
Pelvis	Ijpma et al., 2021 [85]	Patient-specific	10	63	12	1 deep wound infection; 1 plate removal at patients request; 4 patients reported some decrease in physical function after 1 year	
	Merema et al., 2017 [86]	Patient-specific	1	48	3	None	
	Wang et al., 2020 [65]	Patient-specific	15	45.1		1 screw loosening	
		Conventional	35	46.6		1 wound infection; 1 deep vein thrombosis; 1 traumatic arthritis; 2 obturator nerve injuries	
	Wu et al., 2020 [78]	Patient-specific	20	50.1	35.2	None	223
		Conventional	23	51	36.9	None	260
Radius Wrist	Xu et al., 2014 [79]	Patient-specific	24	54.8	30.8	1 preoperative bending; 1 pneumonia; 1 thrombo-embolism; 1 sciatic nerve injury; 1 superficial infection; 1 heterotopic bone ossification	
	Dobbe et al., 2014 [80]	Patient-specific	1	40	20	Pain of scar and surrounding tissue	
	Dobbe et al., 2021 [88]	Patient-specific	10	37	6	3 screw breakage; 4 hardware removal; 1 patient preference for corrective surgery	
	Del Pino et al., 2014 [67]	Patient-specific	5	48	19	None	
	Schindele et al., 2022 [89]	Patient-specific	14	56	12	1 plate removed because of pressure sensitivity; 1 wound dehiscence	92
Humerus	Cao et al., 2023 [90]	Patient-specific	1	14	14	None	
	Sodl et al., 2002 [68]	Patient-specific	5	16.4	26	1 Carpal tunnel syndrome	
	Shuang et al., 2016 [91]	Patient-specific	6	46.2	10.6	None	70
		Conventional	7	40.3		1 poor Mayo elbow performance score	92
Foot	Yao et al., 2021 [46]	Patient-specific	1	24	36	None	
Rib	Ahmed et al., 2021 [92]	Patient-specific	2	27 and 72	16 and 13	None	

The range of Poisson's ratio for the plates reported in the literature varied from 0.3 to 0.35 with a median 0.3.

Geometry is another important factor affecting the biomechanical properties of bone plates. Plate length, width, and thickness all have an impact on plate compliance, interfragmentary strain, and callus formation. A short plate can result in increased stress concentration on both plate and bone, while a longer plate is more compliant and induces callus formation [1, 27, 57]. In addition, a thicker and wider plate generally results in a higher stiffness of the plate [48, 51]. From a clinical point of view, there is a trade-off between the stiffness and stability of the plate and its size, as a smaller plate is preferred to minimize the incision size and reduce the chances of infection of surrounding tissue [42, 60].

Carefully considering the geometry of a patient-specific bone plate can help reduce local stress concentrations on the plate. For example, MacLeod et al. increased the width and thickness of the plate around the screw holes and gave it a slight curve, resulting in a more even distribution of stress over the plate, and a reduction of strain per bone volume [29]. Other studies have investigated optimizing plate properties by using shapes such as a “dog bone” plate or a plate with increasing width from proximal to distal [8, 13, 51].

Different fixation mechanisms are used for bone plate fixation. The DCP is designed to be pressed tightly against the bone using non-threaded screw holes, promoting primarily healing. In contrast, the LP uses threaded screw holes for a secure fixation, resulting in a mechanically stable plate [27, 74, 78]. LPs also allow for an interface distance to promote callus formation and decrease the risk of bone necrosis [20, 22, 54, 66]. In addition, these plates do not require an exact patient-specific fit [22, 54]. LPs are less prone to screw loosening but may lead to prolonged healing [11, 74]. LCPs combine the benefits of both DCP and LP, allowing for compression and stable fixation. They have pre-drilled holes for both non-threaded and threaded screws [49, 74]. For example, Yan et al. designed a plate with locking screws for angular screw fixation, combination holes where both non-locking and locking screws could be used, in a design that allows an interface distance to maximize perfusion and callus forming [54]. Nevertheless, material type should be considered when selecting a fixation mechanism, as it was found that partially removing the threads of a titanium LP improved the plate’s fatigue strength due to notch sensitivity [11, 28]. All three types of fixation mechanisms have been in use in practice, and plate failures and complications exist for each and are comparable [22, 66, 74]. Kimsal et al. conducted a FEA to compare LPs and DCPs and found that an LP could withstand higher loads than a DCP [27]. However, it was not clear if this was a result of the fixation mechanism or the geometrical differences between the plates. LPs are more expensive than DCPs [34], and an optimal fixation mechanism has not been established in literature.

The interface distance refers to the distance between the bone and plate after fixation and is dependent on the anatomical fit of the plate, anatomical location of the fracture, and the type of fixation mechanism used (*e.g.,* LP, DCP or LCP) [20]. A smaller interface distance increases stiffness but interferes with the vascularization of the periosteum, thereby increasing the risk of bone necrosis (20, 38). On the other hand, a larger interface distance increases compliancy, inducing strain at the fracture gap and promoting callus formation [12, 63, 66, 81]. Fixated plates with interface distances smaller than 2.0 mm could withstand the applied mechanical loads [12, 20, 63, 66]. Ahmad et al. and Stoffel et al. reported on plate instability caused by a decline in axial stiffness and torsional rigidity resulting from a 5.0- and 6.0-mm interface distance [37, 66]. Ghimire et al. also found a delayed healing or even a non-union when an interface distance of 4.0 mm was found [63].

Enlarging the working length by removing the screw adjacent to the fracture resulted in a reduction of 64% and 36% of axial stiffness and torsional rigidity, respectively [37, 45, 63, 70]. Every subsequent screw removal reduced axial stiffness and torsional rigidity by an additional 10%. Maximum stress was observed around the screw holes closest to the fracture gap within the plate. By solidifying these screw holes, the working length increases and the stress that was initially concentrated around the holes closest to the fracture gap are now distributed over the whole working length of the plate instead [2, 12, 13, 29, 39, 54, 63]. In addition, the working length must be adjusted to the size of the fracture and the interface distance of the plate, as instability increases with a larger fracture combined with a longer working length, and a larger interface distance requires a smaller working length [63].

Yield strength and stress distribution improved when a triangular or alternating pattern of screws was used [1]. There was no effect on axial stiffness when more than three screws were used proximally and distally from the fracture [37]. Torsional rigidity did not increase with more than four screws on both sides of the fracture.

Conventional plates were compared to 3D printed plates, and the latter showed comparable or increased elastic stiffness, yield strength and hardness [8–10, 26, 42, 65]. In terms of post-processing, *e.g.,* heat treatment of the 3D printed plates was necessary to achieve comparable fatigue strength to conventional plates [8]. Residual stresses in the 3D printed parts can occur because of the 3D printing process. This could affect the fatigue strength of the implant and can also result in warping. Heat treatment can reduce these residual stresses. Furthermore, 3D printed plates need to be polished to remove support structures of the printing and to obtain a smooth surface that prevents infection, friction at bone-plate interface, and bone ingrowth [10, 42]. Despite these positive results, 3D printing technology is still new, and further research is required to evaluate the biomechanical behavior of 3D printed plates and establish optimal parameters (*e.g.,* build orientation, processing protocols, and post-processing techniques) [9, 80, 95]. However, 3D printed patient-specific implants have been used in surgery, with limited postoperative complications [80].

Three studies compared clinical outcomes between patients who received conventional bone plates and those who received patient-specific bone plates [65, 78, 91]. The rate of anatomical reduction was higher in the patient-specific bone plate group, and fewer complications were observed [61, 65, 78]. In addition, patients who underwent surgery with a patient-specific bone plate had a shorter mean operation time. This was attributed to the need for prebending of conventional bone plates during surgery [78, 91].

This review provides an overview of different design parameters for bone plates, but the results should be interpreted carefully for several reasons. The studies included in this literature review did not investigate a single parameter, but rather a combination of parameters to design the desired plate. The variations in the combination of parameters evaluated, challenge the establishment of the effect on biomechanical properties of the plate because of a single parameter. Also, the extend of simplification of boundary conditions in FEA and experimental protocol and setup, varied between studies, which challenges the comparison of outcomes between studies. Furthermore, it is yet unclear to what extent the experimental results are applicable to the clinical setting. The clinical papers showed safe and effective use of patient-specific bone plates [86, 91], but how the experimental findings relate to the clinic is not yet clear. Future studies should aim to establish standard protocols for testing and evaluating patient-specific bone plates to improve their clinical translation.

This paper focused on design parameters for patient-specific bone plates in orthopedic surgery, excluding findings reported by maxillofacial and cranial studies while these disciplines have a lot of experience with bone plate fixations. Also, the effect of screw length and diameter were not included in this study since the focus was on plate properties themselves.

5 Conclusion

The biomechanical properties of bone plates, including elastic stiffness, yield strength, tensile strength, and Poisson's ratio, are determined by a combination of factors, such as material properties, geometry, interface distance, fixation mechanism, screw placement, working length, and manufacturing techniques. This review serves as a useful reference guide for determining which parameters should be adjusted to achieve the desired biomechanical properties of a plate for fixation of a specific type of fracture.

Declarations

Conflict of interest All authors certify that they have no affiliations with or involvement in any organization or entity with any financial interest or non-financial interest in the subject matter or materials discussed in this manuscript. The authors have no financial or proprietary interests in any material discussed in this article.

References

1. Caiti G et al (2019) Biomechanical considerations in the design of patient-specific fixation plates for the distal radius. Med Biol Eng Comput 57(5):1099–1107
2. Chen X (2018) Parametric design of patient-specific fixation plates for distal femur fractures. Proc Inst Mech Eng H 232(9):901–911
3. Manić M et al (2015) Design of 3D model of customized anatomically adjusted implants. Facta Univ Ser: Mech Eng 13(3):269–282
4. Benli S et al (2008) Evaluation of bone plate with low-stiffness material in terms of stress distribution. J Biomech 41(15):3229–3235
5. Fouad H (2010) Effects of the bone-plate material and the presence of a gap between the fractured bone and plate on the predicted stresses at the fractured bone. Med Eng Phys 32(7):783–789
6. Uhthoff HK, Poitras P, Backman DS (2006) Internal plate fixation of fractures: short history and recent developments. J Orhopaedic Sci 11(2):118–126
7. Saidpour SH (2006) Assessment of carbon fibre composite fracture fixation plate using finite element analysis. Ann Biomed Eng 34(7):1157–1163
8. Smith KE et al (2016) Use of 3D printed bone plate in novel technique to surgically correct hallux valgus deformities. Tech Orthop 31(3):181–189
9. Tilton M et al (2020) Additive manufacturing of fracture fixation implants: design, material characterization, biomechanical modeling and experimentation. Addit Manuf 33:101137
10. Liu PC et al (2014) A study on the mechanical characteristics of the EBM-printed Ti-6Al-4V LCP plates in vitro. J Orthop Surg Res 9:106
11. Tseng WJ et al (2016) Notch sensitivity jeopardizes titanium locking plate fatigue strength. Injury 47(12):2726–2732
12. Fan X et al (2018) Parametric study of patient-specific femoral locking plates based on a combined musculoskeletal multibody dynamics and finite element modeling. Proc Inst Mech Eng H 232(2):114–126
13. Chen X, He K, Chen Z (2017) A Novel Computer-Aided Approach for Parametric Investigation of Custom Design of Fracture Fixation Plates. Comput Math Methods Med 2017:7372496
14. Dobbe JG et al (2013) Patient-tailored plate for bone fixation and accurate 3D positioning in corrective osteotomy. Med Biol Eng Comput 51(1–2):19–27
15. Gutwald R, Jaeger R, Lambers FM (2017) Customized mandibular reconstruction plates improve mechanical performance in a mandibular reconstruction model. Comput Methods Biomech Biomed Engin 20(4):426–435
16. Yang WF et al (2018) Three-dimensional printing of patient-specific surgical plates in head and neck reconstruction: A prospective pilot study. Oral Oncol 78:31–36
17. Stokbro K, Bell RB, Thygesen T (2018) Patient-Specific Printed Plates Improve Surgical Accuracy In Vitro. J Oral Maxillofac Surg 76(12):2647.e1-2647.e9
18. Willemsen K et al (2019) Challenges in the design and regulatory approval of 3d-printed surgical implants: a two-case series. Lancet Digit Health 1(4):e163–e171
19. Xie P et al (2017) Comparison of conventional reconstruction plate versus direct metal laser sintering plate: an in vitro mechanical characteristics study. J Orthop Surg Res 12(1):128
20. Petersik A et al (2018) A numeric approach for anatomic plate design. Injury 49(Suppl 1):S96-s101
21. Chen J et al (2023) Biomechanical evaluation of reconstruction of the posterior complex in restorative laminoplasty with miniplates. BMC Musculoskelet Disord 24(1):298
22. Chung C-Y (2018) A simplified application (app) for the parametric design of screw-plate fixation of bone fractures. J Mech Behav Biomed Mater 77(642–648)
23. Freitas A et al (2021) New fixation method for Pauwels type III femoral neck fracture: a finite element analysis of sliding hip screw, L-shaped, and L-shaped with medial plate. Eur J Orthop Surg Traumatol 31(6):1069–1075

24. Gupta SK et al (2021) Enhanced biomechanical performance of additively manufactured Ti-6Al-4V bone plates. J Mech Behav Biomed Mater 119:104552
25. Kaymaz I, et al. (2022) A new design for the humerus fixation plate using a novel reliability-based topology optimization approach to mitigate the stress shielding effect. Clin Biomech 99
26. Kim SJ et al (2017) Biomechanical Properties of 3-Dimensional Printed Volar Locking Distal Radius Plate: Comparison With Conventional Volar Locking Plate. J Hand Surg Am 42(9):747.e1-747.e6
27. Kimsal J et al (2015) Finite element analysis of plate-screw systems used in medial opening wedge proximal tibial osteotomies. Int J Biomed Eng Technol 19(2):154–168
28. Lin CH et al (2018) Modification of the screw hole structures to improve the fatigue strength of locking plates. Clin Biomech (Bristol, Avon) 54:71–77
29. MacLeod AR et al (2018) The effect of plate design, bridging span, and fracture healing on the performance of high tibial osteotomy plates: An experimental and finite element study. Bone Joint Res 7(12):639–649
30. Münch M et al (2022) Stresses and deformations of an osteosynthesis plate in a lateral tibia plateau fracture. Biomed Tech 67(1):43–52
31. Samsami S et al (2022) Biomechanical Comparison of 2 Double Plating Methods in a Coronal Fracture Model of Bicondylar Tibial Plateau Fractures. J Orthop Trauma 36(4):E129–E135
32. Schader JF et al (2022) One size may not fit all: patient-specific computational optimization of locking plates for improved proximal humerus fracture fixation. J Shoulder Elbow Surg 31(1):192–200
33. Shams SF, et al. (2022) The comparison of stress and strain between custom-designed bone plates (CDBP) and locking compression plate (LCP) for distal femur fracture. Eur J Orthop Surg Traumatol
34. Sokol SC et al (2011) Biomechanical properties of volar hybrid and locked plate fixation in distal radius fractures. J Hand Surg Am 36(4):591–597
35. Soni A, Singh B (2020) Design and Analysis of Customized Fixation Plate for Femoral Shaft. Indian J Orthop 54(2):148–155
36. Subasi O et al (2023) Investigation of lattice infill parameters for additively manufactured bone fracture plates to reduce stress shielding. Comput Biol Med 161:107062
37. Stoffel K et al (2003) Biomechanical testing of the LCP–how can stability in locked internal fixators be controlled? Injury 34:11–19
38. Synek A, Baumbach SF, Pahr DH (2021) Towards optimization of volar plate fixations of distal radius fractures: Using finite element analyses to reduce the number of screws. Clin Biomech (Bristol, Avon) 82:105272
39. Reina-Romo E et al (2014) Biomechanical design of less invasive stabilization system femoral plates: computational evaluation of the fracture environment. Proc Inst Mech Eng H 228(10):1043–1052
40. Thomrungpiyathan T et al (2021) A custom-made distal humerus plate fabricated by selective laser melting. Comput Methods Biomech Biomed Engin 24(6):585–596
41. Vancleef S et al (2022) Thin patient-specific clavicle fracture fixation plates can mechanically outperform commercial plates: An in silico approach. J Orthop Res 40(7):1695–1706
42. Wang D, et al. (2017) Customized a Ti6Al4V Bone Plate for Complex Pelvic Fracture by Selective Laser Melting. Materials (Basel) 10(1)
43. Wang J et al (2020) Plating System Design Determines Mechanical Environment in Long Bone Mid-shaft Fractures: A Finite Element Analysis. J Invest Surg 33(8):699–708
44. Wang Y et al (2022) Biomechanical Evaluation of an Oblique Lateral Locking Plate System for Oblique Lumbar Interbody Fusion: A Finite Element Analysis. World Neurosurg 160:e126–e141
45. Wee H et al (2017) Finite Element-Derived Surrogate Models of Locked Plate Fracture Fixation Biomechanics. Ann Biomed Eng 45(3):668–680
46. Yao Y et al (2021) A personalized 3D-printed plate for tibiotalocalcaneal arthrodesis: Design, fabrication, biomechanical evaluation and postoperative assessment. Comput Biol Med 133. https://doi.org/10.1016/j.compbiomed.2021.104368
47. Zhang X, et al. (2019) Finite element analysis of spiral plate and Herbert screw fixation for treatment of midshaft clavicle fractures. Medicine (United States) 98(34)
48. Chakladar ND, Harper LT, Parsons AJ (2016) Optimisation of composite bone plates for ulnar transverse fractures. J Mech Behav Biomed Mater 57:334–346
49. Kanchanomai C, Muanjan P, Phiphobmongkol V (2010) Stiffness and endurance of a locking compression plate fixed on fractured femur. J Appl Biomech 26(1):10–16
50. Murat F, Kaymaz I, Korkmaz IH (2021) A new porous fixation plate design using the topology optimization. Med Eng Phys 92:18–24
51. Olender G et al (2011) A preliminary study of bending stiffness alteration in shape changing nitinol plates for fracture fixation. Ann Biomed Eng 39(5):1546–1554
52. Peleg E et al (2006) A short plate compression screw with diagonal bolts–a biomechanical evaluation performed experimentally and by numerical computation. Clin Biomech (Bristol, Avon) 21(9):963–968
53. Teo AQA et al (2022) Standard versus customised locking plates for fixation of schatzker ii tibial plateau fractures. Injury 53(2):676–682
54. Yan L et al (2020) Finite element analysis of bone and implant stresses for customized 3D-printed orthopaedic implants in fracture fixation. Med Biol Eng Comput 58(5):921–931
55. Kabiri A, G Liaghat, F Alavi (2021) Biomechanical evaluation of glass fiber/polypropylene composite bone fracture fixation plates: Experimental and numerical analysis. Comp Biol Med 132
56. Le C et al (2023) Experimental and numerical investigation of 3D-Printed bone plates under four-point bending load utilizing machine learning techniques. J Mech Behav Biomed Mater 143:105885
57. Nobari S, Katoozian HR, Zomorodimoghadam S (2010) Three-dimensional design optimisation of patient-specific femoral plates as a means of bone remodelling reduction. Comput Methods Biomech Biomed Engin 13(6):819–827
58. Ren W et al (2022) The Study of Biomechanics and Clinical Anatomy on a Novel Plate Designed for Posterolateral Tibial Plateau Fractures via Anterolateral Approach. Front Bioeng Biotechnol 10:818610
59. Sheng X et al (2022) Femoral neck fractures in middle-aged and young adults using femoral neck system assisted by 3D printed guide plate. Chin J Tissue Eng Res 26(33):5290–5296
60. Arnone JC et al. (2013) Computer-aided engineering approach for parameteric investigation of locked plating systems design. J Med Devices 7(2)
61. Ma L et al (2017) 3D printed personalized titanium plates improve clinical outcome in microwave ablation of bone tumors around the knee. Sci Rep 7(1):7626
62. Shin SH, et al. (2022) Does a Customized 3D Printing Plate Based on Virtual Reduction Facilitate the Restoration of Original Anatomy in Fractures? J Pers Med 12(6). https://doi.org/10.3390/jpm12060927
63. Ghimire S et al (2019) Effects of dynamic loading on fracture healing under different locking compression plate configurations: A finite element study. J Mech Behav Biomed Mater 94:74–85
64. Wen X et al (2020) Comparative biomechanical testing of customized three-dimensional printing acetabular-wing plates for complex acetabular fractures. Adv Clin Exp Med 29(4):459–468
65. Wang C et al (2020) Three-dimensional printing of patient-specific plates for the treatment of acetabular fractures involving quadrilateral plate disruption. BMC Musculoskelet Disord 21(1):451
66. Ahmad M et al (2007) Biomechanical testing of the locking compression plate: when does the distance between bone and implant significantly reduce construct stability? Injury 38(3):358–364

67. del Pino JG (2014) A new total wrist fusion locking plate for patients with small hands or with failed partial wrist fusion: preliminary experience. J Wrist Surg 3(2):148–153
68. Sodl JF, Kozin SH, Kaufmann RA (2002) Development and use of a wrist fusion plate for children and adolescents. J Pediatr Orthop 22(2):146–149. https://journals.lww.com/pedorthopaedics/toc/2002/03000
69. Peterson JM et al (2018) Stiffness Matters: Part I-The Effects of Plate Stiffness on the Biomechanics of ACDF In Vitro. Spine (Phila Pa 1976) 43(18):E1061-e1068
70. Märdian S et al (2015) Working length of locking plates determines interfragmentary movement in distal femur fractures under physiological loading. Clin Biomech 30(4):391–396
71. Wang CC et al (2020) Biomechanical analysis of the treatment of intertrochanteric hip fracture with different lengths of dynamic hip screw side plates. Technol Health Care 28(6):593–602
72. Wang L et al (2021) Bone morphological feature extraction for customized bone plate design. Sci Rep 11(1):15617. https://doi.org/10.1038/s41598-021-94924-9
73. Teo AQA et al (2021) Point-of-Care 3D Printing: A Feasibility Study of Using 3D Printing for Orthopaedic Trauma. Injury 52(11):3286–3292
74. Bastias C et al (2014) Are locking plates better than non-locking plates for treating distal tibial fractures? Foot Ankle Surg 20(2):115–119
75. Oraa J, et al. (2023) Derotation tibial osteotomy with custom cutting guides and custom osteosynthesis plate printed with 3D technology: Case and technical note. Annal 3D Print Med 9
76. Gardner MJ et al (2010) Less rigid stable fracture fixation in osteoporotic bone using locked plates with near cortical slots. Injury 41(6):652–656. https://doi.org/10.1016/j.injury.2010.02.022
77. Jo WL et al (2023) Structural analysis of customized 3D printed plate for pelvic bone by comparison with conventional plate based on bending process. Sci Rep 13(1):10542
78. Wu H-Y et al (2020) Personalized three-dimensional printed anterior titanium plate to treat double-column acetabular fractures: A retrospective case-control study. Orthop Surg 12(4):1212–1222
79. Xu M et al (2014) Custom-made locked plating for acetabular fracture: a pilot study in 24 consecutive cases. Orthopedics 37(7):e660–e670
80. Dobbe JG et al (2014) Patient-specific distal radius locking plate for fixation and accurate 3D positioning in corrective osteotomy. Strateg Trauma Limb Reconstr 9(3):179–183
81. Brodke DS et al (2001) Dynamic cervical plates: biomechanical evaluation of load sharing and stiffness. Spine (Phila Pa 1976) 26(12):1324–9
82. Sharma S, Mudgal D, Gupta V (2023) Advancement in biological and mechanical behavior of 3D printed poly lactic acid bone plates using polydopamine coating: Innovation for healthcare. J Mech Behav Biomed Mater 143:105929
83. Hwang BY, Lee JW (2020) Lingual Application of Pre-Bent Reconstruction Plate for Segmental Mandibular Defect: Easy and Accurate Method Through the Buccal Drilling Approach Using Computer-Aided Design/Computer-Aided Manufacturing Surgical Guides. J Craniofac Surg 31(3):851–852
84. Jeong SH et al (2022) Patient-specific high tibial osteotomy for varus malalignment: 3D-printed plating technique and review of the literature. Eur J Orthop Surg Traumatol 32(5):845–855. https://doi.org/10.1007/s00590-021-03043-8
85. Ijpma FFA et al (2021) Feasibility of Imaging-Based 3-Dimensional Models to Design Patient-Specific Osteosynthesis Plates and Drilling Guides. JAMA Netw Open 4(2):e2037519
86. Merema BJ et al (2017) The design, production and clinical application of 3D patient-specific implants with drilling guides for acetabular surgery. Injury 48(11):2540–2547
87. Edelmann A, M Dubis, R Hellmann (2020) Selective Laser Melting of Patient Individualized Osteosynthesis Plates-Digital to Physical Process Chain. Materials (Basel) 13(24)
88. Dobbe JGG et al (2021) Patient-specific plate for navigation and fixation of the distal radius: a case series. Int J Comput Assist Radiol Surg 16(3):515–524
89. Schindele S, et al. (2022) Three-Dimensionally Planned and Printed Patient-Tailored Plates for Corrective Osteotomies of the Distal Radius and Forearm. J Hand Surg Am
90. Cao C et al (2023) Three-dimensional printing designed customized plate in the treatment of coronal fracture of distal humerus in teenager: A case report. Medicine (Baltimore) 102(2)
91. Shuang F et al (2016) Treatment of Intercondylar Humeral Fractures With 3D-Printed Osteosynthesis Plates. Medicine (Baltimore) 95(3). https://doi.org/10.1097/md.0000000000002461
92. Ahmed ADB, Prakash PS, Li Cynthia CM (2021) Customized 3-dimensional printed rib plating in chest wall reconstruction. JTCVS Tech 8:213–215
93. Liu B et al (2022) Experimental study of a 3D printed permanent implantable porous Ta-coated bone plate for fracture fixation. Bioact Mater 10:269–280. https://doi.org/10.1016/j.bioactmat.2021.09.009
94. Fan H et al (2021) Highly Porous 3D Printed Tantalum Scaffolds Have Better Biomechanical and Microstructural Properties than Titanium Scaffolds. Biomed Res Int 2021:2899043
95. Das S, Bourell DL, Babu SS (2016) Metallic materials for 3D printing. MRS Bull 41(10):729–741

Publisher's note Springer Nature remains neutral with regard to jurisdictional claims in published maps and institutional affiliations.

S. G. Brouwer de Koning Due to interests in physics and mathematics, together with medicine, Susan Brouwer de Koning studied Technical Medicine at the University of Twente. She graduated with distinction from the master track 'Medical imaging and interventions' after spending a year in London, UK, for her graduation project at the Research Oncology department of Guy's and St Thomas' hospital in association with King's College London. Due to her interest in intra-operative imaging technologies, she began working at the Netherlands Cancer Institute, Antoni van Leeuwenhoek, as a PhD student and as a member of the Clinical Implementation Team that guides the implementation of innovations in the surgical workflow. To be more involved with the patient rather than a role solely as a researcher, she entered the graduate entry program in medicine with a strong focus on research, at the VU University, Amsterdam, during the last years of her PhD. Next to her clinical rotations, she is still doing research at the 3DLab of the OLVG, to implement 3D printed clinical devices into the clinical workflow.

N. de Winter Medical engineer

V. Moosabeiki A mechanical design engineer with expertise in computational mechanics, mechanical behavior of materials, computer-aided technologies (CAD/CAM/CAE), manufacturing design and process

M.J. Mirzaali Assistant professor at Delft University of Technology with expertise in amongst others, 3D printing, metamaterials and biomaterials

A. Berenschot Medical librarian, information specialist

M.M.E.H. Witbreuk Orthopedic surgeon

V. Lagerburg Medical physicist